17th World Conference on Earthquake Engineering, 17WCEE
Sendai, Japan - September 13th to 18th 2020

SHAKE TABLE TESTS OF PRECAST COLUMNS WITH GEOPOLYMER CONCRETE SEGMENTS REINFORCED WITH BFRP BARS

H. Hao[1], C. Li[2], K. Bi[3]

[1] *John Curtin Distinguished Professor, Curtin University, hong.hao@curtin.edu.au*
[2] *Research Associate, Curtin University, chao.li11@postgrad.curtin.edu.au*
[3] *Senior Lecturer, Curtin University, kaiming.bi@curtin.edu.au*

Abstract

Geopolymer concrete has been developed as a green material to replace the ordinary Portland cement concrete so as to reduce the carbon dioxide emissions. On the other hand, researches on using basalt fibre reinforced polymer (BFRP) bars to replace steel reinforcements have been carried out recently to minimize corrosion damages of the steel bars in the conventional concrete structures. Prefabricated construction can minimize the on-site construction activities and the related environmental impact, and it is becoming more and more popular in the construction industry. Combining these emerging new materials and construction methods could result in an environmentally friendly, durable and sustainable infrastructure system. The seismic behavior of this novel system is however not clear. This study experimentally investigated the seismic performances of precast segmental columns with geopolymer concrete reinforced with BFRP bars through shake table tests. Both uniaxial and biaxial ground motions were used as inputs. It was found that the BFRP reinforced geopolymer concrete segmental column had comparable performance to the steel reinforced normal concrete segmental column. The column under biaxial seismic excitations experienced more damages in the segments than that of the column under uniaxial excitation.

Keywords: Precast segmental column; shake table tests; geopolymer concrete; BFRP bars

1. Introduction

Cast-in-place constructions of steel reinforced concrete structures have been used for many years in the construction industry around the world. As most steps of this construction method such as formwork preparation, steel cages fixing and concrete casting are finished on site, a variety of disadvantages have been observed in the past practices. For instance, the cast-in-place construction is time consuming and often cause traffic disruption due to the large amount of on-site construction work. Moreover, the construction quality of the structure and the safety for the construction workers are not easy to control due to the complex on-site conditions. Furthermore, the environmental impacts of the cast-in-place construction such as dust and water pollution are unavoidable. To solve these challenges, precast construction has been proposed and is now attracting more and more attentions due to its numerous advantages [1].

As one type of the precast structures, precast segmental column has been used as the substructure of bridges. However, most of the applications of precast segmental column are limited in the areas with low seismicity due to the concern of its seismic performance [2]. Many studies have been carried out to investigate the seismic performance of precast segmental column in order to widen its application [3-9]. It was generally found that the posttensioned segmental column has better self-centring capacity than the traditional cast-in-place monolithic column [8, 10]. However, openings might occur at the joints between the segments when the segmental column is subjected to lateral cyclic loading and cause concrete crushing damages near the joints [2, 5]. In order to mitigate such damage, different methods have been proposed in previous studies. For example, Chou and Chen used steel tube to confine the segments [4], ElGawady et al. adopted FRP tubes to confine the concrete [8], and some other researchers used high performance fibre reinforced concrete to minimize the crushing damages [3, 11]. Another characteristic of segmental column is that, compared to the monolithic column, the precast segmental column has limited energy dissipation capacity [10]. In order to increase the energy dissipation capacity of the precast segmental column, different energy dissipation devices have been proposed, including internal and external energy dissipation devices. For instance, Ou et al. adopted internal mild steel bars as the energy dissipation devices and it was found that the internal energy devices were effective to increase energy dissipation capacity of the column [5, 12]. However, it should be noted that it is difficult to replace the internal energy dissipation devices after major earthquakes. Therefore, some other researchers proposed external energy dissipation devices. For example, Mashal and Palermo designed the external dissipater which was made of steel bars encased in a tube and used them in the precast bridge bent [13].

Ordinary Portland cement (OPC) has been used for many years and is still widely utilised in current construction industry. The manufacturing of cement normally consists of calcination process, which can result in large amount of carbon dioxide emission. It is reported that the cement industry contributes around 5-7% of the global carbon dioxide emission [14-18]. To address this concern, environmentally friendly concrete binders have been proposed. Geopolymer concrete (GPC) is a cementless binder which consists of aluminosilicate material and alkaline liquids [16, 19]. The commonly used aluminosilicate material includes fly ash and slag. Since these materials are industrial byproducts, both the carbon dioxide emission and cost of the geopolymer concrete are lower than conventional cement-based concrete [15]. Therefore, the geopolymer concrete could be a good alternative to the cement-based concrete considering its economic and environmental advantages.

Steel bar corrosion normally causes cracks in concrete and it is one of the major reasons that cause deterioration of steel reinforced structures. In order to address this problem, the application of fibre reinforced polymer bars (FRP bars) has attracted increasing attention [20-22]. Compared to steel bars, the FRP bars have higher strength, lower unit weight and higher corrosion resistance [23]. Commonly used FRPs include carbon FRP, glass FRP and aramid FRP. Recently, basalt FRP (BFRP) is becoming an appealing alternative to other FRPs due to its lower cost and good strength and stiffness [24, 25]. Other advantages of BFRP include high temperature resistance and good resistance to corrosion and alkali condition [26]. Due to these advantages, the applications of BFRP is becoming more and more popular. In the present study, BFRP rebars were used to replace the traditional steel rebars.

It should be noted that most previous studies on precast segmental columns focused on its quasi-static performance [3-9], very limited studies examined its dynamic performances. Motaref et al. [27] and Moustafa et al. [28] carried out shaking table tests on the precast segmental column and investigated its seismic performance recently. However, only uniaxial excitation was considered in these tests. In reality, an earthquake ground motion has three components. Very recently, the authors carried out shake table tests and biaxial lateral excitations were used in the tests [29]. However, it should be noted that only segment columns with steel reinforced OPC were tested. No previous study reported the seismic performance of segmental column with BFRP reinforced GPC. In the present study, shaking table tests were performed to examine the behaviours of segmental column with BFRP reinforced GPC. Both the uniaxial and biaxial earthquake ground motions were considered. For comparison, the performances of segmental column made from normal steel reinforced OPC were also tested.

2. Experimental program

2.1 Test specimens

The prototype column is a bridge pier with a height of 7.32m and a diameter of 1.22m. Considering the capacity of the shake table system in the structural dynamics lab at Curtin University, the prototype column was scaled down with a scaling factor of 12. As a result, the height and diameter of the column were 600mm and 100mm, respectively. Table 1 shows the scaling factors of the tested column. Fig. 1 shows the designs of the test specimen which include the column, footing, cap, base slab and top mass. Three segmental columns were designed and constructed. All the three columns had the same dimensions and the differences were the materials used for the segments and the loading scheme during the tests. The first column S1 was a column with OPC and steel reinforcement. In the second column S2, GPC and BFRP bars were used instead of OPC and steel bars. Both S1 and S2 were subjected to bidirectional earthquake motions. The column S3 was identical with the second column S2, but the column was subjected to a uniaxial earthquake motion instead of biaxial inputs. The column itself had three identical segments with a height of 200mm each. In each segment, four longitudinal bars with a diameter of 6mm were used and the stirrups had a diameter of 3mm and a spacing of 35mm. As shown in Fig. 1, the segments, footing and cap were clamped together with a posttensioned steel tendon. The tendon that used to clamp the segments had a diameter of 9.3mm. The initial posttension force Table 2 shows the mixed design of the OPC and GPC. The measured compressive strength of the OPC and GPC were 49.8 MPa and 48.5 MPa, respectively. The designed posttension force was 28kN which was around 0.073 $f_c A_g$, in which f_c is the concrete compressive strength, A_g is the gross sectional area of the column. The ultimate strength of the posttension tendon was 1860 MPa, therefore, the initial posttension force was around 28% of the tensile capacity of the tendon. The material properties of the steel and BFRP bars are shown in Table 3.

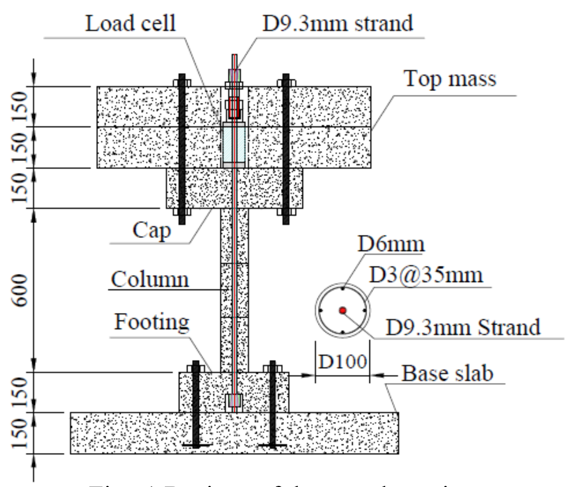

Fig. 1 Designs of the tested specimen

Table 1 Scaling factors [29]

Physical Quantities			Scale Factors, S_i Scale rule	Values
Geometry	Length of superstructure	l	S_l	12
	Displacement	δ	S_l	12
Material properties	Modulus of elasticity	E	S_E	1
	Stress	σ	S_E	1
	Strain	ε	1	1
	Poisson's Ratio	v	1	1
Dynamic properties	Acceleration	α	S_a	1
	Mass	m	$S_E S_l^2/S_a$	144
	Frequency	ω	$(S_a/S_l)^{0.5}$	0.29
	Velocity	v	$(S_l S_a)^{0.5}$	3.46
	Time	t	$(S_l/S_a)^{0.5}$	3.46
Loadings	Force	F	$S_E S_l^2$	144
	Moment	M	$S_E S_l^3$	1728

Table 2 Mixed design of concrete (kg/m^3)

Mixed concrete	Aggregates	Sand	Cement	Fly ash	Slag	Water	Na_2SiO_3 solution	NaOH solution
OPC	863	876	408	-	-	204	-	-
GPC	1196	644	-	360	40	-	173.7	59.4

Table 3 Material properties

Material	Diameter mm	Elastic modulus (GPa) Steel/BFRP	Yield strength (MPa) Steel/BFRP	Ultimate strength (MPa) Steel/BFRP
Longitudinal rebar	6	200/55	555/-	616/1100
Stirrup	3	200/55	346/-	430/1100
Steel tendon	9.3	195	1674	1860

2.2 Test setup

As mentioned above, the column, footing and cap were clamped together first by applying posttensioning force in the tendon. Considering the capacity of the shake table, four shake tables were combined and controlled simultaneously to form a large table in this study. A base block was used as the support for the specimen. The base concrete block was fixed to the shake tables first and then the footing of the specimen was tied to the base concrete block with four bolts. After installing the column, the top mass was aligned and fixed to the cap of the column. Accelerometers and LVDTs were installed to measure the responses of the tested specimens during the experiments. Fig. 2 shows the layout of the sensors and Fig. 3 shows a photo of the final setup of the test.

The tested columns were subjected to bidirectional or uniaxial earthquake motions. The original data were records from Niland Fire Station during the 1979 Imperial Valley Earthquake. In the test, the original earthquake motions were scaled and the maximum PGA (peak ground acceleration) was gradually increased from 0.1g up to the failure of the column with an interval of 0.1g. Considering the scaling factor of the column and following the similitude law as shown in Table 1, the time duration of the inputs was compressed by $\sqrt{12} = 3.46$ times. Fig. 4 shows the input motions in the two directions with a maximum PGA of 0.1g in the E-W direction. For column S3 under uniaxial excitation, the input was the component in the E-W direction as shown in Fig. 4 (b).

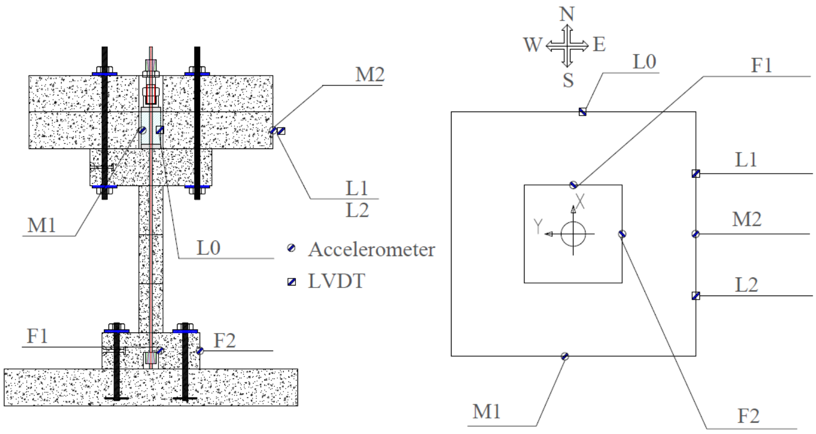

Fig. 2. Layout of the sensors

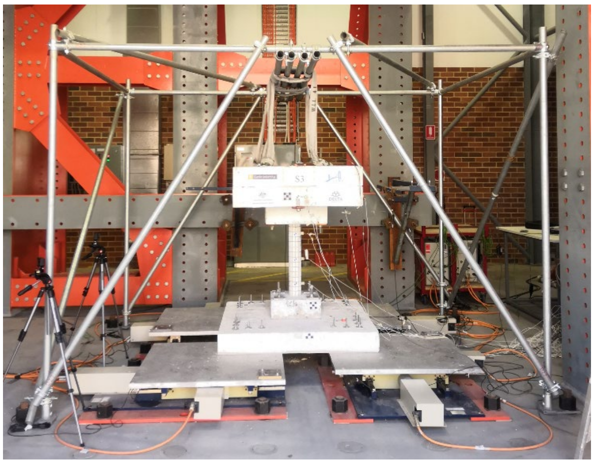

Fig. 3 Final setup of the test

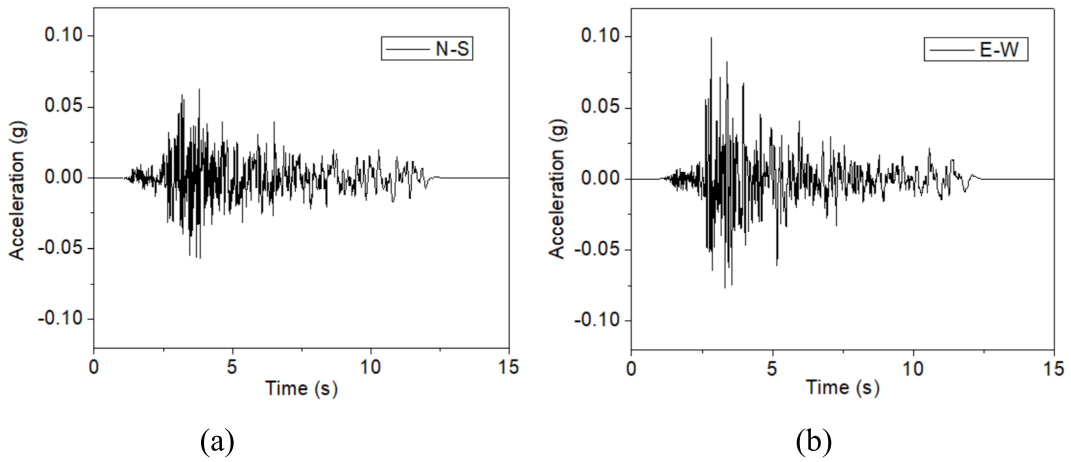

Fig. 4 A pair of the biaxial input motions with a maximum PGA of 0.1g: (a) N-S, (b) E-W

3. Experimental results

3.1. Observed damages

Columns S1 and S2 both collapsed at the PGA of 0.9g and the column S3 at 1.1g. Fig. 5 shows the damage patterns of the three columns. It can be observed that the damages of the three segmental columns were mainly concentrated at the joint between the column and the footing. Comparing Figs. 5(a) and (b), it can be found that the damage regions of S1 and S2 were similar, which indicated that the BFRP reinforced GPC column had similar performance as compared to the steel reinforced OPC column in resisting seismic ground motions. S2 and S3 were designed to investigate the effect of biaxial excitation. As shown in Figs. 5(b) and (c), more damages were observed in the column under biaxial excitations (S2) and the damages were distributed at the toes of the column in both the loading directions (N-S and E-W). For the column under uniaxial loading (S3), the damages were located at the joint in the E-W direction only (where the loading was applied). The coupling effect of the biaxial excitations caused more damages in S2, resulting in the collapse of the column at the PGA of 0.9g.

Column	Observed damages
S1	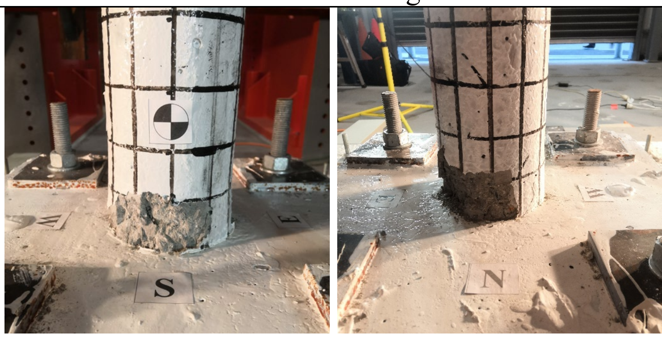 (a)
S2	 (b)
S3	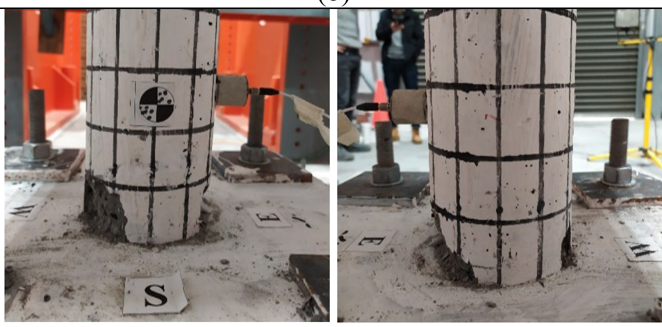 (c)

Fig. 5 Damages of the three columns

3.2 Variation of periods

Before each earthquake input, white noise tests were carried out to identify the vibration characteristics of the columns. Fig. 6 shows the changes of the first vibration periods of the three specimens.

As shown in Fig. 6 (a), columns S1 and S2 had similar vibration periods before the test (see the results when PGA=0.1g). Before the PGA reached 0.5g, minor increase was found for both columns, indicating that the damage of the two columns was insignificant. After 0.5g, the vibration periods of column S1 started to increase significantly, especially in the E-W direction. This could be because the PGA of the input in this direction was larger than that in the N-S direction as shown in Fig. 4, which in turn resulted in the more severe damage in this direction. For column S2, the vibration periods started to increase obviously after the PGA reached 0.6g. Fig. 6 (a) also shows that the increment in vibration period of column S2 was slower than that of S1 with the increase of PGA. This could be attributed to the better confinement provided by the BFRP stirrups as the strength of the BFRP was larger than the steel bars [26]. Therefore, the use of geopolymer concrete and BFRP reinforcement could be a good alternative to the normal steel reinforced concrete in the precast segmental column. For columns S2 and S3, as shown in Fig. 6 (b), the vibration periods of the columns were similar and did not increase significantly at small PGA. After the PGA reached 0.6g, the vibration period of column S2 started to increase obviously as mentioned above, while for column S3 it started to increase after the PGA reached 0.7g. This indicates that column S2 experienced more damage during the tests in comparison with column S3. This is consistent with the observed damage as shown in Fig. 5 and discussion in section 3.1.

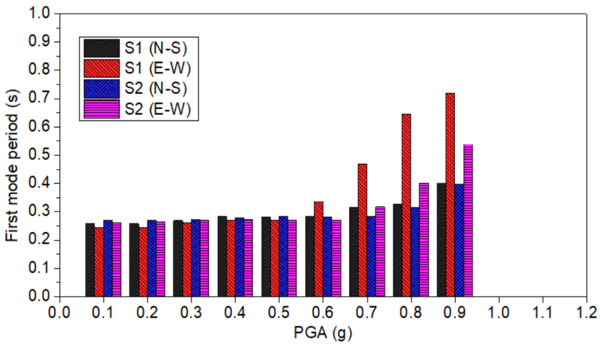

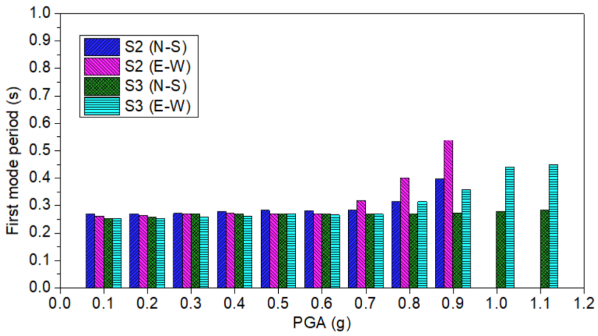

Fig. 6 fundamental periods of: (a) S1 and S2; (b) S2 and S3 (prior to each test)

3.3 Displacements

The absolute displacements of the columns were obtained from the LVDTs. By subtracting the displacements of the shake table, the relative displacements of the column can be calculated. For column S1, since the LVDTs were affected by the swinging wires unexpectedly during the tests when the PGAs were 0.7g and 0.8g, the results were therefore not compared here. Fig. 7 shows the relative displacements of the three columns when the PGAs were 0.2g, 0.4g and 0.6g. According to Figs. 7 (a) and (b), the displacement responses of columns S1 and S2 at the PGA of 0.2g were similar. For columns S2 and S3, as shown in Figs. 7 (c) and (d), the displacement responses of S2 and S3 in the E-W direction were also close to each other. In the N-S direction, for column S3, it still had small displacements though there was no input in this direction. This might be because of the twisting of the column. As the stiffness center and mass center could not be exactly coincident in the real construction due to the construction and assembling error, the input motion could induce torsional moment and cause twisting of the column. When the PGA reached 0.4g, the displacement responses of columns S1 and S2 were compared in Figs. 7 (e) and (f). Again, the displacements of the two columns were almost the same in both directions. For columns S2 and S3, the displacement responses were shown in Figs. 7 (g) and (h). The results were similar to those when the PGA was 0.2g. When the PGA reached 0.6g, the displacement responses of columns S1 and S2 are shown in Figs. 7 (i) and (j). It can be observed that the displacement of S1 in the N-S direction increased significantly after about 10s, indicating the column experienced severe damages. However, for column S2, the displacements were still quite small. This could be attributed to the better confinement provided by the BFRP stirrups as explained above. Figs. 7 (k) and (l) show the displacement responses of columns S2 and S3. In the N-S direction, S2 experienced larger displacement responses due to the biaxial input motions. As shown in Fig. 7 (l), in the E-W direction, the displacement responses of S2 and S3 were similar from the beginning to around 9s. After this, the displacement amplitude of S2 became larger than that of S3. This is because of the biaxial excitations and coupling effect of the input caused more accumulated damages in the column, resulting in larger responses as shown in the test results.

PGA	N-S	E-W
0.2g	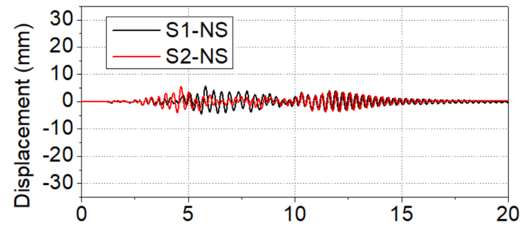	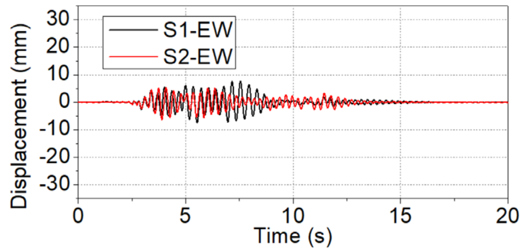
	(a)	(b)
	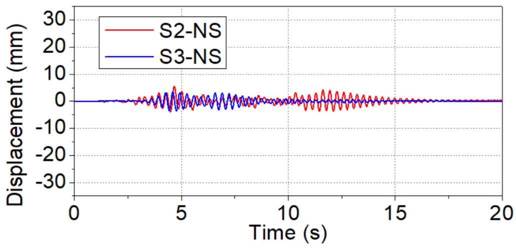	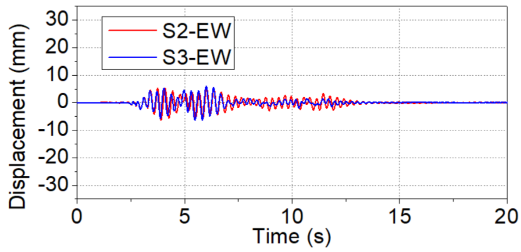
	(c)	(d)
0.4g	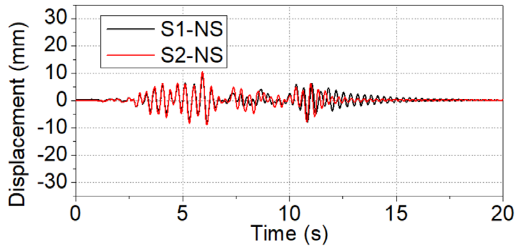	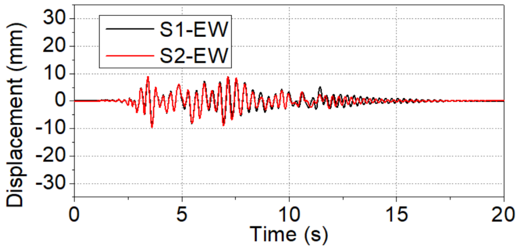
	(e)	(f)
	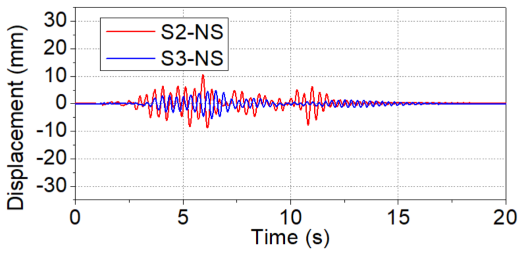	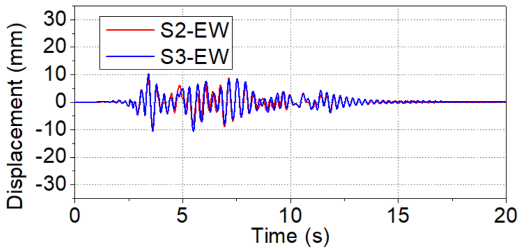
	(g)	(h)

PGA	N-S	E-W
0.6g	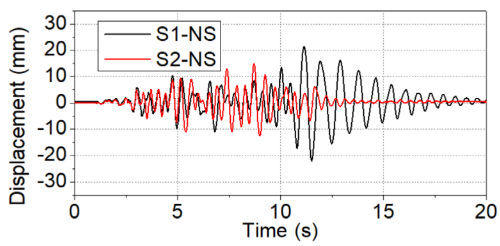	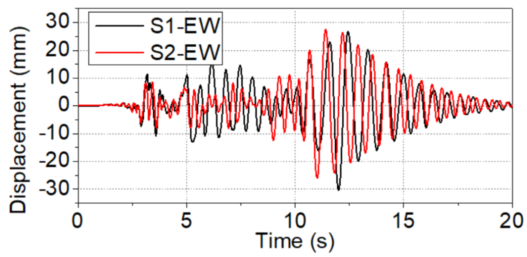
	(i)	(j)
	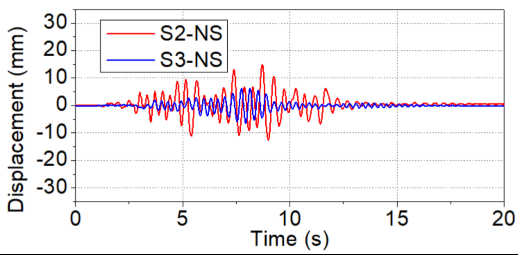	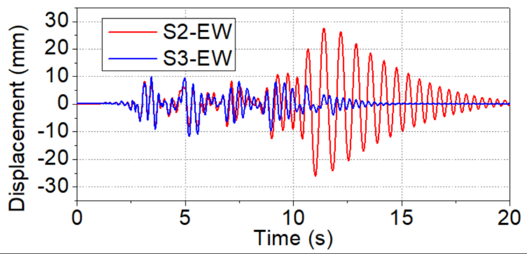
	(k)	(l)

Fig. 7 Displacement responses of the columns

4. Conclusions

In this study, shake table tests were carried out to investigate the seismic performance of precast segmental column with GPC segments reinforced with BFRP bars. For comparison, the behaviors of the normal segment columns with steel reinforced OPC were also tested. The influences of the biaxial and uniaxial inputs on the performances of the precast segmental columns were also investigated. According to the test results, the column with BFRP reinforced GPC segments had similar performance under small to medium levels of excitations compared to the steel reinforced concrete. When the PGAs reached large values, the column with BFRP reinforced geopolymer concrete segments performed slightly better owing to the more evident confinement provided by the BFRP bars. For the columns under uniaxial and biaxial excitations, the effect of the biaxial excitations had limited influence on the responses of the column at small to medium excitations. However, once significant damages occurred to the column when the column was subjected to large PGAs, the coupling effect of the biaxial excitations resulted in more damages in the segments, causing faster increases of vibration period and larger displacement responses. More damages in the segments also resulted in the earlier collapse of the column.

4. Acknowledgements

The authors acknowledge the financial support from Australia Research Council. The authors would like to thank Mr. Ashley Hughes, Dr. Haoran Zuo, Dr. Tin V. Do for their help during the test.

6. References

[1] Kurama YC, Sritharan S, Fleischman RB, Restrepo JI, Henry RS, Cleland NM et al. (2018): Seismic-Resistant Precast Concrete Structures: State of the Art. *Journal of Structural Engineering,* **144**(4), 03118001-03118001.

[2] Wang JC, Ou YC, Chang KC, Lee GC. (2008): Large-scale seismic tests of tall concrete bridge columns with precast segmental construction. *Earthquake Engineering & Structural Dynamics,* **37**(12), 1449-1465.

[3] Billington SL, Yoon J. (2004): Cyclic response of unbonded posttensioned precast columns with ductile fiber-reinforced concrete. *Journal of Bridge Engineering,* **9**(4), 353-363.

[4] Chou CC, Chen YC. (2006): Cyclic tests of post-tensioned precast CFT segmental bridge columns with unbonded strands. *Earthquake Engineering & Structural Dynamics,* **35**(2), 159-175.

[5] Ou YC, Wang PH, Tsai MS, Chang KC, Lee GC. (2009): Large-scale experimental study of precast segmental unbonded posttensioned concrete bridge columns for seismic regions. *Journal of Structural Engineering,* **136**(3), 255-264.
[6] Li C, Hao H, Bi K. (2017): Numerical study on the seismic performance of precast segmental concrete columns under cyclic loading. *Engineering Structures,* **148**, 373-386. doi:https://doi.org/10.1016/j.engstruct.2017.06.062
[7] Li C, Hao H, Zhang X, Bi K. (2017): Experimental study of precast segmental columns with unbonded tendons under cyclic loading. *Advances in Structural Engineering,* **21**(3), 319-334.
[8] ElGawady M, Booker AJ, Dawood H. (2010): Seismic behavior of posttensioned concrete-filled fiber tubes. *Journal of Composites for Construction,* **14**(5), 616-628.
[9] Shim CS, Lee S, Park S, Koem C. (2017): Experiments on prefabricated segmental bridge piers with continuous longitudinal reinforcing bars. *Engineering Structures,* **132**, 671-683. doi:http://dx.doi.org/10.1016/j.engstruct.2016.11.070
[10] Bu ZY, Ou YC, Song JW, Zhang NS, Lee GC. (2015): Cyclic Loading Test of Unbonded and Bonded Posttensioned Precast Segmental Bridge Columns with Circular Section. *Journal of Bridge Engineering*, 04015043.
[11] Zhang Y, Fan W, Zhai Y, Yuan W. (2019): Experimental and Numerical Investigations on Seismic Behavior of Prefabricated Bridge Columns with UHPFRC Bottom Segments. *Journal of Bridge Engineering,* **24**(8), 04019076.
[12] Ou YC, Tsai MS, Chang KC, Lee GC. (2010): Cyclic behavior of precast segmental concrete bridge columns with high performance or conventional steel reinforcing bars as energy dissipation bars. *Earthquake Engineering & Structural Dynamics,* **39**(11), 1181-1198.
[13] Mashal M, Palermo A. (2019): Low-Damage Seismic Design for Accelerated Bridge Construction. *Journal of Bridge Engineering,* **24**(7), 04019066.
[14] Mo KH, Alengaram UJ, Jumaat MZ. (2016): Structural performance of reinforced geopolymer concrete members: A review. *Construction and Building Materials,* **120**, 251-264. doi:10.1016/j.conbuildmat.2016.05.088
[15] McLellan BC, Williams RP, Lay J, Van Riessen A, Corder GD. (2011): Costs and carbon emissions for geopolymer pastes in comparison to ordinary portland cement. *Journal of Cleaner Production,* **19**(9-10), 1080-1090.
[16] Singh B, Ishwarya G, Gupta M, Bhattacharyya SK. (2015): Geopolymer concrete: A review of some recent developments. *Construction and Building Materials,* **85**, 78-90. doi:10.1016/j.conbuildmat.2015.03.036
[17] Maranan GB, Manalo AC, Benmokrane B, Karunasena W, Mendis P. (2016): Behavior of concentrically loaded geopolymer-concrete circular columns reinforced longitudinally and transversely with GFRP bars. *Engineering Structures,* **117**, 422-436. doi:10.1016/j.engstruct.2016.03.036
[18] Ma C-K, Awang AZ, Omar W. (2018): Structural and material performance of geopolymer concrete: A review. *Construction and Building Materials,* **186**, 90-102. doi:10.1016/j.conbuildmat.2018.07.111
[19] Elchalakani M, Dong M, Karrech A, Li G, Mohamed Ali MS, Manalo A. (2018): Behaviour and design of air cured GFRP-reinforced geopolymer concrete square columns. *Magazine of Concrete Research*, 1-63. doi:10.1680/jmacr.17.00534
[20] De Luca A, Matta F, Nanni A. (2010): Behavior of full-scale glass fiber-reinforced polymer reinforced concrete columns under axial load. *ACI Structural Journal,* **107**(5), 589.
[21] Hadi MNS, Karim H, Sheikh MN. (2016): Experimental Investigations on Circular Concrete Columns Reinforced with GFRP Bars and Helices under Different Loading Conditions. *Journal of Composites for Construction,* **20**(4). doi:10.1061/(asce)cc.1943-5614.0000670
[22] Asim N, Alghoul M, Mohammad M, Amin MH, Akhtaruzzaman M, Amin N et al. (2019): Emerging sustainable solutions for depollution: Geopolymers. *Construction and Building Materials,* **199**, 540-548. doi:10.1016/j.conbuildmat.2018.12.043
[23] Maranan GB, Manalo AC, Benmokrane B, Karunasena W, Mendis P. (2015): Evaluation of the flexural strength and serviceability of geopolymer concrete beams reinforced with glass-fibre-reinforced polymer (GFRP) bars. *Engineering Structures,* **101**, 529-541. doi:10.1016/j.engstruct.2015.08.003
[24] Monaldo E, Nerilli F, Vairo G. (2019): Basalt-based fiber-reinforced materials and structural applications in civil engineering. *Composite Structures,* **214**, 246-263. doi:10.1016/j.compstruct.2019.02.002
[25] Dal Lago B, Taylor SE, Deegan P, Ferrara L, Sonebi M, Crosset P et al. (2017): Full-scale testing and numerical analysis of a precast fibre reinforced self-compacting concrete slab pre-stressed with basalt fibre reinforced polymer bars. *Composites Part B: Engineering,* **128**, 120-133. doi:10.1016/j.compositesb.2017.07.004
[26] Fan X, Zhang M. (2016): Behaviour of inorganic polymer concrete columns reinforced with basalt FRP bars under eccentric compression: An experimental study. *Composites Part B: Engineering,* **104**, 44-56. doi:10.1016/j.compositesb.2016.08.020
[27] Motaref S, Saiidi MS, Sanders D. (2013): Shake table studies of energy-dissipating segmental bridge columns. *Journal of Bridge Engineering,* **19**(2), 186-199.

[28] Moustafa A, ElGawady MA. (2018): Shaking Table Testing of Segmental Hollow-Core FRP-Concrete-Steel Bridge Columns. *Journal of Bridge Engineering,* **23**(5), 04018020.
[29] Li C, Bi K, Hao H. (2019): Seismic performances of precast segmental column under bidirectional earthquake motions: Shake table test and numerical evaluation. *Engineering Structures,* **187**, 314-328. doi:10.1016/j.engstruct.2019.03.001